Tumbling through a landscape: Evidence of instabilities in high-dimensional moduli spaces

Brian Greene, David Kagan, Ali Masoumi, Dhagash Mehta, Erick J. Weinberg, and Xiao Xiao

Phys. Rev. D **88**, 026005 — Published 9 July 2013

DOI: 10.1103/PhysRevD.88.026005

Tumbling through a landscape: Evidence of instabilities in high-dimensional moduli spaces

Brian Greene,[1,*] David Kagan,[2,†] Ali Masoumi,[1,‡]
Dhagash Mehta,[3,§] Erick J. Weinberg,[1,¶] and Xiao Xiao[1,**]

[1]*Physics Department, Columbia University, New York, New York 10027, USA*

[2]*Department of Physics, University of Massachusetts Dartmouth, North Dartmouth MA 02747, USA*

[3]*Department of Physics, Syracuse University, Syracuse, NY 13244, USA*

We argue that a generic instability afflicts vacua that arise in theories whose moduli space has large dimension. Specifically, by studying theories with multiple scalar fields we provide numerical evidence that for a generic local minimum of the potential the usual semiclassical bubble nucleation rate, $\Gamma = A\, e^{-B}$, increases rapidly as function of the number of fields in the theory. As a consequence, the fraction of vacua with tunneling rates low enough to maintain metastability appears to fall exponentially as a function of the moduli space dimension. We discuss possible implications for the landscape of string theory. Notably, if our results prove applicable to string theory, the landscape of metastable vacua may not contain sufficient diversity to offer a natural explanation of dark energy.

*Electronic address: greene@phys.columbia.edu
†Electronic address: dkagan@umassd.edu
‡Electronic address: ali@phys.columbia.edu
§Electronic address: dbmehta@syr.edu
¶Electronic address: ejw@phys.columbia.edu
**Electronic address: xx2146@columbia.edu

I. INTRODUCTION

The discovery that string theory admits an enormous number of flux vacua [1–3] has played a formative role in the theory's development for well over a decade. Aspects of these vacua, from their phenomenological and cosmological properties to their distribution and statistical features, have been extensively studied [4, 5]. Yet, due to the complexity of this landscape of vacua, many basic questions remain. In this paper we undertake a study, pursued from a variety of perspectives in a number of works [6–13], that is of potential relevance to one such vital question: Do we expect these vacua to be long-lived? As a direct analysis would present formidable challenges, we instead consider generic, field theoretic models of the landscape and study how the stability of vacua varies as the dimension of the moduli space (the number of fields) increases. Our results suggest that tunneling rates, and hence vacuum instability, grow so rapidly with the number of moduli that the probability of a given local minimum being metastable is exponentially small.

In field theory, vacuum decay by quantum tunneling was studied by Coleman [14, 15]. He showed that the decay proceeded by the nucleation of bubbles of a lower vacuum inside the original false vacuum. In the semiclassical approximation the nucleation rate per unit volume is governed by a bounce solution of the Euclidean field equations. It can be written in the form $\Gamma = Ae^{-B}$, where A depends on the determinant of fluctuations around the bounce solution and B is the Euclidean action of the bounce. The analysis was extended to include gravitational effects by Coleman and De Luccia [16]. For decay from a de Sitter vacuum the resulting corrections to the nucleation rate are typically small unless the potentials are Planckian in scale or the bubbles nucleate with a size comparable to the horizon length. With unusually flat potential barriers it can happen that there is no Coleman-De Luccia bounce, but in such cases there is always a Hawking-Moss [17] solution corresponding to a process in which an entire horizon volume fluctuates to the top of the potential barrier.

In string theory the large number of vacua and moduli fields complicates the situation, but at the same time opens up lines of attack based on statistical analysis. For example, Denef and Douglas [18] proposed a method of calculating the density of flux vacua in the string landscape in terms of the Kähler potential on the moduli space of a given Calabi-Yau compactification. Their work showed that a sharp accumulation of vacua generally occurs near the conifold locus in moduli space. Dine et al. [8] used scaling arguments to conclude

that vacua in the string landscape with small cosmological constant become unstable when fluxes are large relative to their compactification volume. Chen et al. [19] and Marsh et al. [20] showed that increasing the number of moduli fields suppresses exponentially the chance that a randomly chosen critical point will be a minima, with the suppression growing for vacua with high energy.

In this paper we also pursue a statistical approach, focusing our analysis on effective field theory models of many-dimensional moduli spaces. We provide numerical evidence that the rate for tunneling out of a typical false vacuum grows rapidly as a function of the number of moduli fields. Specifically, the fraction of vacua with tunneling rates low enough to maintain metastability appears to fall as an exponential of a power of the moduli space dimension.

In Sec. II we describe our approach for estimating tunneling rates in field theoretical models of high-dimensional moduli spaces. Our numerical methods and results are described in Sec. III. These results reveal a general feature of high-dimensional field theories and are independent of applications to the string landscape. In Sec. IV we discuss the efficacy of using random potentials to model the string landscape, and emphasize various considerations that would need to be resolved before a direct application could be justified. In Sec. V we estimate the maximum dimension of moduli spaces whose associated flux landscape would be expected to generically contain metastable vacua, assuming that our numerics and extrapolations are applicable. The result is a drastic reduction in the number of metastable vacua. Finally, in Sec. VI we suggest future directions for studying these models and summarize our conclusions.

II. VACUUM DECAY

We consider the dynamics of a moduli space spanned by N scalar fields ϕ_j with a Lagrangian

$$\mathcal{L} = \frac{1}{2}\sum_{j=1}^{N} \partial_\mu \phi_j \partial^\mu \phi_j - V(\phi_1, \phi_2, \ldots, \phi_N)\,. \tag{2.1}$$

The potential V will in general have many local minima that correspond to metastable false vacua. Let us consider one of these which, by a shifting of the field variables, can be taken to lie at the origin of field space, $\phi = 0$. Assuming the potential to be smooth at this point,

we can expand it in a power series

$$V = \lambda \left(\sum_i A^{(2)}_{ii} \phi_i^2 v^2 + \sum_{ijk} A^{(3)}_{ijk} \phi_i \phi_j \phi_k v + \sum_{ijkl} A^{(4)}_{ijkl} \phi_i \phi_j \phi_k \phi_l + ... \right) . \tag{2.2}$$

Here v, with dimensions of mass, is a characteristic distance in field space that corresponds to a typical distance between stationary points of V. We have also extracted a dimensionless constant λ, to be chosen so that the dimensionless coefficients of the power series in brackets are of order unity. Finally, we have used the freedom to make an O(N) transformation on the fields to eliminate off-diagonal terms in the quadratic term of the power series.

The exponent B in the bubble nucleation rate is the action of the Euclidean bounce solution. We ignore gravitational effects and assume O(4) symmetry, with the fields being functions only of $s = \sqrt{\mathbf{x}^2 + x_4^2}$. The bounce then satisfies

$$\frac{d^2\phi_j}{ds^2} + \frac{3}{s}\frac{d\phi_j}{ds} = \frac{\partial V}{\partial \phi_j} . \tag{2.3}$$

The boundary conditions are that $\phi(\infty) = 0$, its false vacuum value, and that $\phi'(0) = 0$. The actual value of the field at the origin is not determined in advance, but must be a point on the opposite side of the potential barrier from the false vacuum. Note that, except in the thin-wall limit, $\phi(0)$ is never equal to the true vacuum value.

We will consider large ensembles of potentials, with the coefficients in the power series chosen randomly, as described in more detail in the next section. Ideally, we would calculate the nucleation rate for each potential by solving the bounce equations. However, finding bounce solutions in a theory with more than one scalar field is a daunting numerical problem. Doing so for a large sample of potentials is clearly infeasible. Instead, we invoke a more easily calculable proxy that can provide an indication of how the decay rate varies with the number of fields.

A bounce solution may be viewed as containing a wall region, in which the fields pass through the barrier in $V(\phi)$, and an interior region where the fields are close to their values in the new vacuum. The distinction between the two regions becomes exact in the thin-wall approximation, which is valid in the limit where ϵ, the difference between the energy densities of the true and false vacua, tends to zero. In this approximation the fields in the interior region take on exactly their true vacuum values. The radius R of the bounce is determined by a balance between the negative action in the bounce interior and the positive action in

the wall. With a single scalar field, this wall action is the product of the three-dimensional area of bounce and a surface tension that is well approximated by

$$\sigma = \left| \int_{\phi_{\rm fv}}^{\phi_*} d\phi \, \sqrt{2[V(\phi) - V_{\rm fv}]} \right| , \tag{2.4}$$

where ϕ_* denotes the point on the true vacuum side of the barrier such that $V(\phi_*) = V_{\rm fv}$. With additional scalar fields, σ is obtained by integrating along a path in field space running from the false vacuum to a point near the true vacuum, with the path and endpoint chosen to minimize the integral.

The net result is that $R = 3\sigma/\epsilon$, while the tunneling exponent is

$$B = \frac{\pi^2}{2}\sigma R^3 = \frac{27\pi^2\sigma^4}{2\epsilon^3} \, . \tag{2.5}$$

Thus, in the rare cases in which we have two almost degenerate vacua, the thin-wall approximation is applicable, B is large, bubble nucleation is greatly suppressed, and the false vacuum is long-lived. Since our focus is on effects that enhance bubble nucleation, this approximation is not of direct interest to us. Nevertheless, we can draw some useful insight from it. Equation (2.5) shows a strong dependence on ϵ. This cannot continue outside the thin-wall approximation, because then the field in the bounce solution never reaches the true vacuum, and so cannot be directly sensitive to the value of ϵ. On the other hand, the surface tension is closely related to the form of the potential barrier and should continue to be relevant.

Outside the thin-wall limit, the boundary between the wall and the bounce interior is not well defined. A reasonable prescription would be to take it to be the hypersurface in Euclidean space on which $V(\phi)$ is equal to its false vacuum value. We could then define a quantity σ as before, with the integration path running from the false vacuum to a point on the hypersurface Σ in field space, lying on the other side of the potential barrier, on which $V(\phi) = V_{\rm fv}$. The path and the specific endpoint on Σ would be chosen to minimize the integral.

Unfortunately, performing the required minimization for a large ensemble of potentials is still calculationally infeasible. However, a plausible approximation is at hand. We might expect the minimizing path to pass though the region in field space where the barrier in $V(\phi)$ is lowest. This suggests considering a straight-line path running from $\phi = 0$, though each saddle point, $\phi_{\rm sp}$, on the surrounding barrier, and ending on Σ. In fact, since on average the

contributions from the segments before and after the saddle point will be equal, we follow a slightly simpler approach. We integrate over only the first part of the path, extract factors of λ and v, and define the line integral

$$\begin{aligned} \tilde{\sigma} &= 2 \int_P d\phi \, \sqrt{2[V(\phi) - V(0)]} \\ &\equiv \sqrt{\lambda}\, v^3 \, \tilde{s} \,, \end{aligned} \tag{2.6}$$

where P is a straight-line path in field space running from the false vacuum at $\phi = 0$ to the saddle point. There may be many saddle points, and thus many such paths. We expect the tunneling rate to be controlled by the path with the lowest tunneling integral, and define the corresponding value of $\tilde{s}$ to be

$$\tilde{s}_{\rm min} = s \,. \tag{2.7}$$

Standard scaling arguments show that B is inversely proportional to λ, but independent of v, although v does affect the prefactor A in Γ. Outside the thin-wall limit, the typical bounce radius is $R \sim k(\sqrt{\lambda}\, v)^{-1}$, where k is a numerical factor of order unity. This suggests that

$$B \sim \pi^2 R^3 \tilde{\sigma} \sim \frac{\pi^2}{\lambda} \, k^3 \, s \,, \tag{2.8}$$

where we have included a factor of π^2 because of the four-dimensional spherical symmetry. A simple test of this estimate can be obtained by numerically evaluating B and s for a single-field potential with cubic and quartic terms. Inserting the results into Eq. (2.8) and taking v to be half the difference between the true and false vacuum values of ϕ, one obtains values of k that vary between 5.2 and 6.0 over a wide range of parameters away from the thin-wall limit. This suggests

$$B \sim 10^3 \, \frac{s}{\lambda} \,. \tag{2.9}$$

The dilute-gas approximation that underlies the semiclassical approach to bubble nucleation breaks down when B is comparable to or less than unity. In this regime the metastability of the false vacuum has essentially disappeared. The numerical studies that we describe in the next section show that when many scalar fields are present, the overwhelming majority of potentials lead to a value of B too small to maintain metastability with any plausible value of λ.

III. NUMERICAL STUDIES

We numerically studied ensembles of theories with potentials of the form of Eq. (2.2), using s as an indicator of the vacuum stability. To make the calculations manageable we truncated the power series at the quartic terms. An ensemble was defined by taking the $A^{(n)}$ to be random numbers uniformly distributed over ranges defined by

$$\begin{aligned} A^{(2)}_{ii} &\in [0, a_2]\,, \\ A^{(3)}_{ijk} &\in [-a_3, a_3]\,, \\ A^{(4)}_{ijkl} &\in [-a_4, a_4]\,. \end{aligned} \tag{3.1}$$

Allowing the $A^{(4)}_{ijkl}$ to be negative means that the truncated potential is not necessarily bounded from below. This is not a concern for us, since we are only concerned with the behavior near the minimum; at larger distances higher-order terms can provide a lower bound on V.

Because we will be comparing theories with different numbers of fields, an important issue is how to vary the a_n as the number of fields is varied. To determine this, let us require that the typical variation of the potential in a ball of radius ϕ_R in field space be independent of N, the number of fields. This ensures that, for any number $N_0 \leq N$, we can recover results for $N - N_0$ fields by considering an N_0-dimensional cross section of the analysis for N fields. In turn, this ensures that dependencies we find on N are not due to peculiar N-dependent normalizations in V.

With this assumption, the typical value for each of the ϕ_j in such a ball of radius ϕ_R is of order $\phi_R/\sqrt{N}$. The quadratic term is a sum of positive contributions and will be independent of N if a_2 is. There are N^3 cubic terms, each of magnitude $\phi_R^3/N^{3/2}$. Because these can be of either sign, they will tend to cancel, so that the effective number of terms is of order $N^{3/2}$ and we are led to take a_3 to also be N-independent. A similar argument shows that a_4 should also be independent of N.

As for the actual values of the a_n, note that a change of any two of these can be absorbed by a redefinition of λ and v. Hence, there is no loss of generality in taking $a_2 = a_3 = 1$. We did so, and also set $a_4 = 1$; the effect of other choices for a_4 is described below.

For a given value of N we chose an ensemble of 10,000 potentials. For each potential we

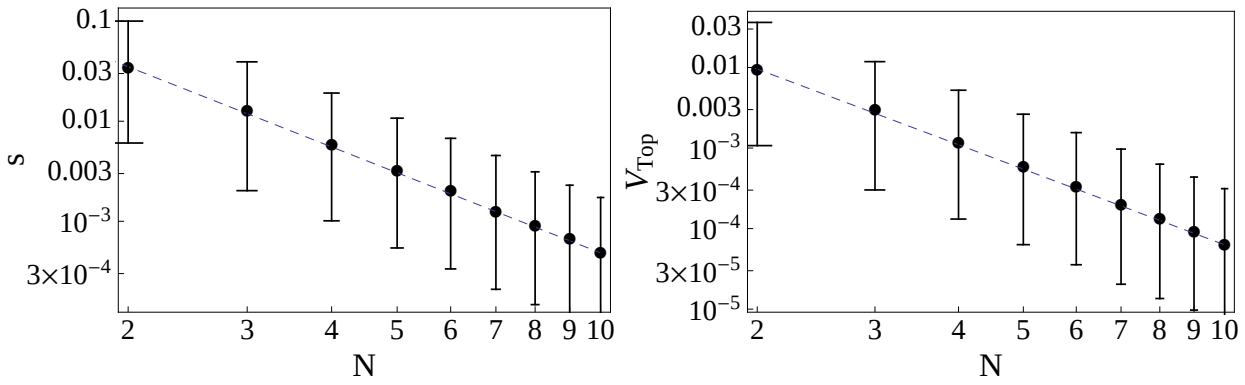

FIG. 1: Left, the median value of s for quartic potentials. Right, the median value of the lowest saddle point, in units of λv^4, for quartic potentials. In both cases the bars indicate the range from the 25th to the 75th percentile.

found all of the stationary points[1] and picked out the saddle points with a single negative mode. From among the saddle points for each potential we found the one that gave the smallest value of $\tilde{s}$ (i.e., $\tilde{s}_{\rm min} \equiv s$) and the one that gave the lowest barrier height. Figure 1 shows the median values of these quantities within each ensemble as functions of N for the quartic potential. For both quantities a sharp decrease with increasing N is clearly evident. Not only do the height and surface tension of these saddle points decrease, but also they get closer to the false vacuum minimum at the origin. This can be seen in Fig. 2, where we have plotted the median distance to the saddle point with lowest $\tilde{s}$. (A plot of median distance to the lowest saddle point is virtually indistinguishable.) All of these plots show a power law dependence on N with, e.g.,

$$s_{\rm median} \approx C_{\rm tension}\, N^{-\alpha_{\rm tension}} \,. \tag{3.2}$$

The best fit values for the various α and C are shown in Table I.

We have also plotted the number of stationary points around the false vacuum, in Fig. 3. These do not follow a power law, but are instead closer to an exponential behavior.

Our decision to arbitrarily terminate the expansion of the potential with the quartic terms was motivated by considerations of calculational practicality. As a test of this choice, we also carried out the calculations without the quartic terms in the potential, retaining only

[1] For a description of the numerical method for finding all such points, see [21]. Further details will be published elsewhere [22].

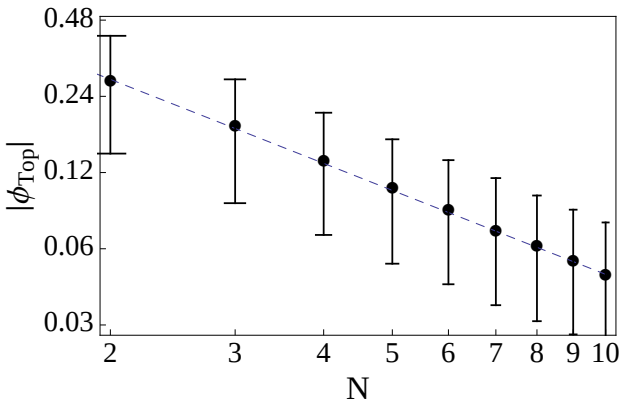

FIG. 2: The median distance, in units of v, to the saddle point with $\tilde{s}_{\rm min} = s$ for quartic potentials. Again, the bars indicate the range from the 25th to the 75th percentile.

	$\alpha_{\rm tension}$	$\alpha_{\rm height}$	$\alpha_{\rm distance}$
Cubic potentials	2.73	3.16	1.15
Quartic potentials	2.66	3.12	1.10
SUSY	3.16	3.99	1.19

	$C_{\rm tension}$	$C_{\rm height}$	$C_{\rm distance}$
Cubic potentials	0.26	0.090	0.67
Quartic potentials	0.22	0.083	0.60
SUSY	0.25	0.11	0.60

TABLE I: Best fit parameters, defined as in Eq. (3.2), for power law fits to the data in Figs. 1, 2, 4, and 5, as well as to the data for the supersymmetric potentials discussed in Sec. IV.

the quadratic and cubic terms. As can be seen from the plots in Figs. 4-6. and the data in Table I, the results are quite similar to those with the quartic term included. This leads us to conclude that our omission of quintic and higher terms has little effect on our results.

We now return to the question of the dependence of the results on the ranges chosen for the coefficients in the potential. As noted previously, any change in the constants defining the ranges of the quadratic and cubic terms can be compensated by a rescaling of λ and v. The dependence on the quartic coefficient range is illustrated in Fig. 7, where we plot the

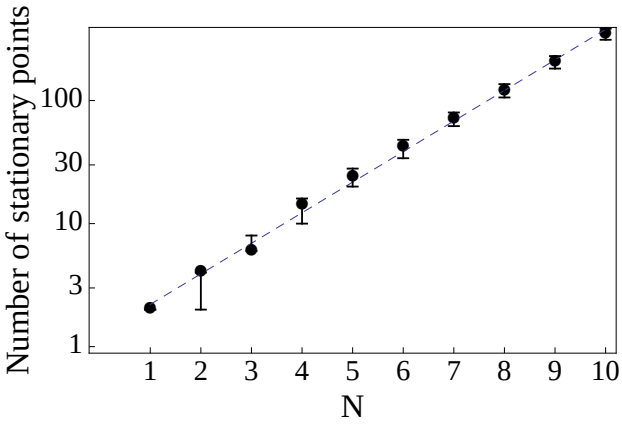

FIG. 3: The median number of saddle points for quartic potentials, with the bars indicating the range from the 25th to the 75th percentile.

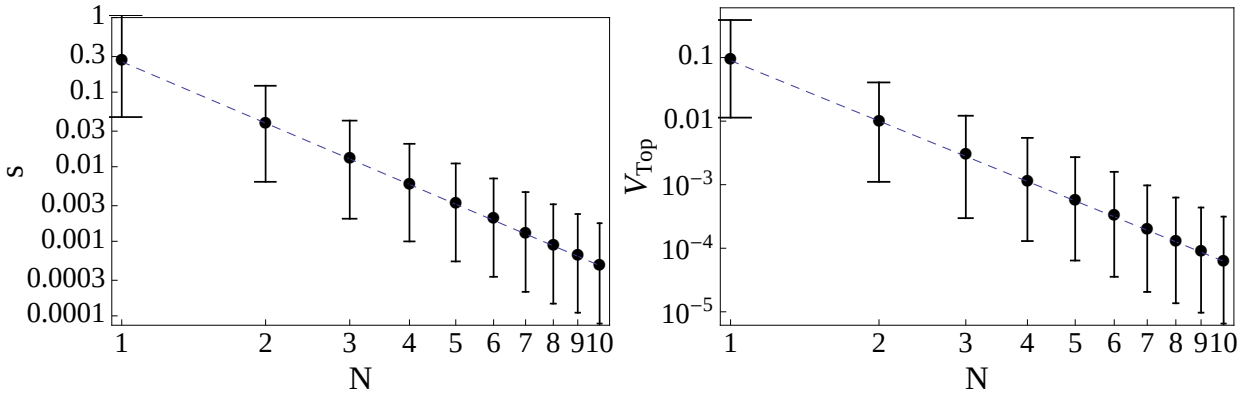

FIG. 4: The same as in Fig. 1, but for cubic potentials.

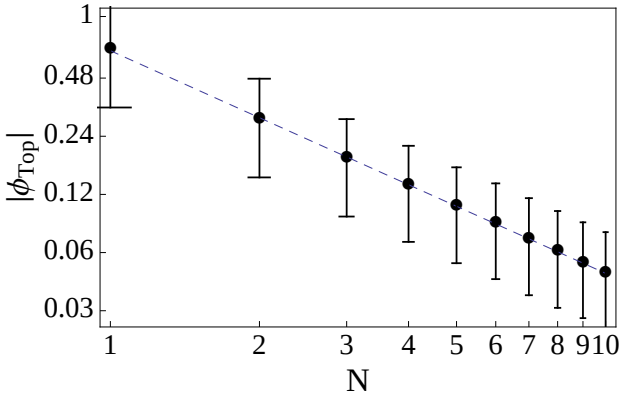

FIG. 5: The same as in Fig. 2, but for cubic potentials.

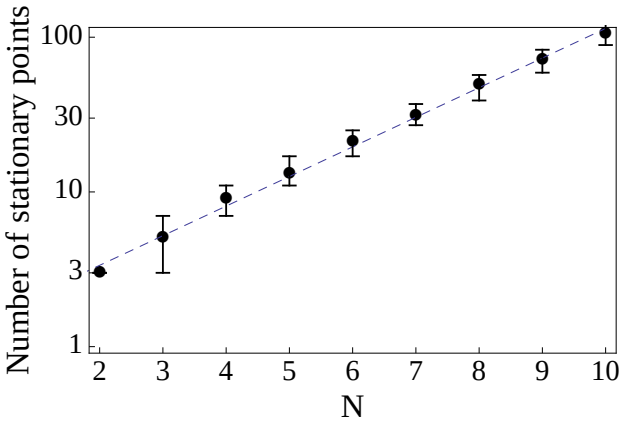

FIG. 6: The same as in Fig. 3, but for cubic potentials.

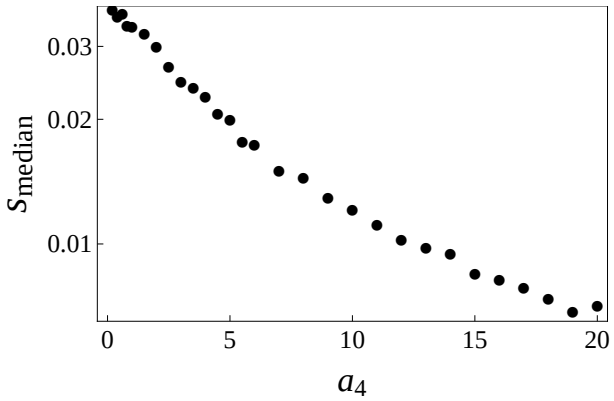

FIG. 7: The dependence of the median value of s on the range parameter a_4. The data shown are for $N = 2$.

median value of s as a function of a_4 with $N = 2$. We see that increasing a_4 produces a roughly exponential decrease in the median value of s; decreasing a_4 to zero simply reduces to the purely cubic potential. Hence the net effect of increasing the range for a_4 would be to lead to a lower tunneling exponent, thus strengthening the effects that we find. The results for the other quantities and other values of N give similar results.

Our data indicate that the median value of s falls rapidly as the number of fields is increased. From this we can conclude that at large N the typical local minimum is less likely to have a low nucleation rate and a long lifetime. This by itself does not tell us about the number of outliers, vacua with high values of s. To study this we examined the distributions of the quantities that we have plotted within a given ensemble. For example, in Fig. 8 we show the distributions of values of s for several choices of N with a quartic

potential. These roughly coincide when they are plotted as functions of $s/s_{\rm median}$. The data suggest that the frequency of large s has an approximately exponential falloff that can be described by

$$n(s) \approx n_0 \exp\left(-\gamma s/s_{\rm median}\right) . \tag{3.3}$$

The values of γ for various values of N are shown in Table II. Similar results are found for the data on the height of and distance to the lowest saddle point.

N	Cubic	Quartic	SUSY
1	0.58	0.46	0.45
2	0.38	0.39	0.33
3	0.40	0.35	0.33
4	0.34	0.33	0.32
5	0.37	0.35	0.32
6	0.37	0.34	
7	0.38	0.34	
8	0.38	0.35	
9	0.38	0.37	
10	0.35	0.34	

TABLE II: Best fit values for the parameter γ in the distributions of surface tension s for cubic and quartic non-supersymmetric and quartic supersymmetric potentials with various N.

Inserting the fit of Eq. (3.2) for $s_{\rm median}$ into this expression gives

$$n(s) \approx n_0 \exp\left(-\frac{\gamma}{C_{\rm tension}} N^\alpha s\right) , \tag{3.4}$$

where for convenience we have defined $\alpha \equiv \alpha_{\rm tension}$. Extrapolating to larger N and using the estimate in Eq. (2.9) suggests that the fraction of potentials with a tunneling exponent greater than some value $\hat{B}$ is roughly

$$f(\hat{B}) \sim \exp(-\beta\, N^\alpha\, \hat{B}) , \tag{3.5}$$

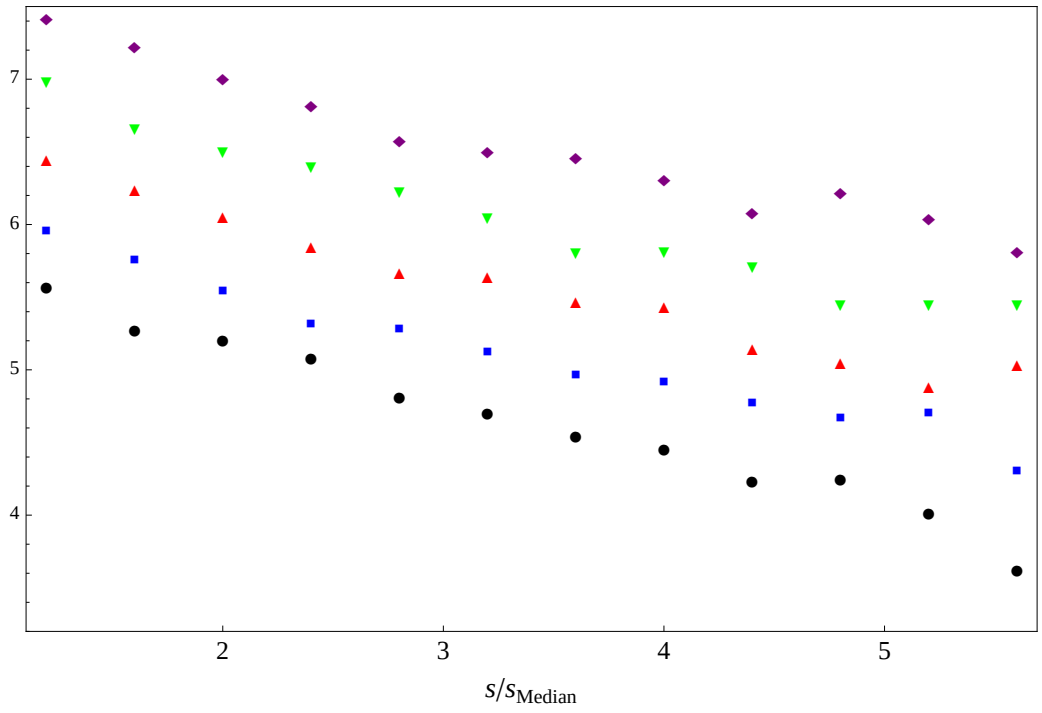

FIG. 8: The distribution of values of s in the ensembles for a quartic potential with various values of N. The vertical axis represents the natural logarithm of the number of values in each bin. For the sake of clarity, the data for different values of N have been offset by constants, so only the slopes are meaningful. Purple diamonds correspond to $N = 2$; green down-pointing triangles, $N = 4$; red up-pointing triangles, $N = 6$; blue squares, $N = 8$; and black circles, $N = 10$.

where

$$\beta = 10^{-3} \frac{\gamma\lambda}{C_{\text{tension}}} \,. \tag{3.6}$$

Our numerical results suggest that $\gamma/C_{\text{tension}}$ is close to unity. Because λ is extracted from the shape of the landscape, there is no reason to expect it to be a small coupling constant. It could well be of order unity, in which case $\beta \sim 10^{-3}$. Equation (3.5) then represents a tremendous suppression with increasing N of vacua with nucleation rates low enough to maintain metastability.

Note that we have ignored gravitational effects in our analysis of tunneling rates. With low barriers and rapid bubble nucleation this is generally a good approximation. It should be noted, though, that in a de Sitter vacuum with a relatively flat barrier the Hawking-Moss bounce provides an alternative mode of vacuum decay. The corresponding decay exponent

is

$$B_{\rm HM} = \frac{3}{8G_N^2}\,\frac{V_{\rm barr}-V_{\rm fv}}{V_{\rm barr}V_{\rm fv}}\,, \tag{3.7}$$

where $V_{\rm fv}$ and $V_{\rm barr}$ are the values of the potential in the false vacuum and at the top of the barrier, while G_N is Newton's constant. Our numerical studies indicate that the barrier height relative to the false vacuum (i.e., $V_{\rm barr}-V_{\rm fv}$) has a power law falloff with N quite similar to that found in the effective wall tension s, thus implying a similar enhancement of the Hawking-Moss transition rate.

IV. POSSIBLE IMPLICATIONS FOR THE STRING LANDSCAPE

The results we have described so far are a general feature of quantum field theories. Our motivation for studying random multi-field potentials, however, is the landscape of string theory. In this section, therefore, we assess the applicability and implications of our findings for the string landscape.

Not only does the enormous number of local minima in the high dimensional string theory landscape (which can serve as the endpoints of tunneling events) offer the possibility of significant enhancement of tunneling probabilities,[2] but we have also seen that such large numbers of fields result in the exponential suppression of tunneling barriers. The question we now briefly consider is the extent to which the random potentials we have analyzed in the previous sections provide accurate insight into properties of the string landscape.

For definiteness, focus on a standard flux compactification of type IIB string theory on a Calabi-Yau manifold M. With $G = F - \tau H$, F and H the RR and NS-NS three-form fluxes, and τ the axio-dilaton, the Gukov-Vafa-Witten superpotential W is given by [24]

$$W = \int G \wedge \Omega\,, \tag{4.1}$$

where Ω is the holomorphic 3-form on M. The associated flux potential V is given by

$$V_M = e^K (D_\rho W D^\rho \overline{W} - 3|W|^2)\,. \tag{4.2}$$

[2] The density of vacua near the conifold point, $\rho_{\rm conifold}$, in a one-dimensional moduli space is described by $1/[r^2(C+\log r)^2]$, where r is the distance from the conifold point [18]; applying this result near a generic point along the conifold locus in an n-dimensional moduli space shows the rapid growth in the number of vacua, $\int d^n r\,\rho_{\rm conifold}$, with n.

Assume that G, together with additional contributions (e.g. D3-brane instantons or wrapped D7-branes), stabilizes all moduli [23]. Then consider $\{V_M\}$ as M varies among all Calabi-Yau's, G varies over flux values, the Kähler stabilizing contributions vary over all possibilities, and supersymmetry-breaking effects similarly scan a broad range. With all such variations in play, the local minima of $\{V_M\}$ will sweep through a large class of vacua. In the vicinity of any such vacuum state, we can expand the effective potential, yielding a field theory model of the form (2.2). Now, considering all such expansions that arise from all local minima of the collection $\{V_M\}$, we expect the expansion coefficients to randomly vary. Indeed, such random variation inspired the ansatz we chose in our numerical studies. But in applying the results of the previous sections to the string landscape, there are a number of details and complications that deserve further attention.

First, we have assumed that the action for tunneling trajectories is well approximated by our proxy: twice that of a straight line in field space connecting the minima being studied and the optimal saddle point on the surrounding barrier. Yet, tunneling trajectories in multidimensional field spaces are notoriously subtle and can exhibit unexpected features; explicit examples in the landscape are the conifunneling trajectories between monodromy-related flux vacua found in [25] (see also [26, 27]). An additional, and potentially pivotal, complication is that the different flux vacua that are not monodromy related are generally minima of distinct potentials. Physically, such transitions invoke features not captured by our local field theoretic model, including for example the nucleation of branes to absorb changes in flux [28, 29]. These effects might significantly affect the tunneling action, and possibly mitigate the field theory instabilities we have identified.

Second, we have assumed that as the stabilizing contributions to a given model are varied the effective potentials around local minima will have expansions that are well modeled by random polynomials. Is this correct? To be concrete, consider the part of the potential arising from the flux, G. On a given Calabi-Yau, M, there are dim $H^3(M)$ fluxes that enter G. As those fluxes vary, we have far fewer free parameters than the coefficients in Eq. (2.2). However, the associated minima of V will occur at different locations, p, in the moduli space of M. As the holomorphic form Ω depends on p, the coefficients in a local expansion of the superpotential, Eq. (4.1), and the corresponding potential, Eq. (4.2), will also vary with p. So, the local potential will be randomized both by the varying fluxes and by the varying values of the period vector over the moduli space. It seems reasonable to us that this will

result in local expansions well modeled by the random potentials invoked in Sec. III, but we do not have a firm argument. We will return to this issue in a forthcoming work, where we will explicitly check this for specific Calabi-Yau's with low-dimensional moduli spaces.

Third, we have taken a canonical form for the kinetic terms in our field theoretic models. It is well known, however, that string vacua are densest in the vicinity of the conifold locus, where the classical moduli space metric suffers from a curvature singularity. In particular, near a generic point on the conifold locus we can choose local coordinates $(Z^1, Z^2, \ldots, Z^P)$ on the moduli space such that $Z^1 = 0$ labels the conifold. Near $Z^1 = 0$, the moduli space metric G behaves as:

$$G^{11}(Z) \sim \ln(|Z^1|^2)\,. \tag{4.3}$$

The local form of the action then takes the form

$$\int \sqrt{-g}[g^{\mu\nu} G_{ij}\,\partial_\mu Z^i\,\partial_\nu Z^j - V(Z)], \tag{4.4}$$

where g is the space-time metric. In this expression the coordinates Z are the moduli space representation of the scalar fields ϕ and V is their flux potential. At any non-singular point we can, of course, use a local change of field variables to absorb G into the Z, yielding a canonical kinetic term. But as we approach a conifold point, this change of variables corresponds to reducing the barrier heights in V (assuming V is continuous and is being expanded about a local minimum) and thus increases tunneling rates. In the regions of moduli space that are most densely populated with string vacua, we therefore expect the non-canonical kinetic terms to augment the destabilization we have found.

Fourth, since the flux potential V is derived from the superpotential W, and it is W that directly incorporates flux values, a more accurate representation of the landscape arises from randomly varying coefficients in a local expansion of W, and then using the result to calculate the random potentials. In principle, the relationships between the coefficients in V, which reflect its origin in W, could alter our findings.

We have undertaken such an analysis. Specifically, we considered a theory with N chiral superfields Φ_j. The superpotential W was taken to be a polynomial

$$W = \frac{1}{2}\sum_i C^{(2)}_{ii}\Phi_i^2 + \frac{1}{3}\sum_{ijk} C^{(3)}_{ijk}\Phi_i\Phi_j\Phi_k + \frac{1}{4}\sum_{ijkl} C^{(4)}_{ijkl}\Phi_i\Phi_j\Phi_k\Phi_l + ... \tag{4.5}$$

The $C^{(2)}_{ii}$ were randomly chosen real numbers in the range $[0,1]$, while $C^{(3)}_{ijk}$ and $C^{(4)}_{ijkl}$ were complex numbers whose real and imaginary parts were taken randomly from the interval $[-1,1]$. The scalar field potential derived from W was then truncated at quartic order and analyzed in a fashion similar to our non-supersymmetric potentials. With up to $N = 5$ superfields we again find a power law falloff with N. Because the N chiral superfields correspond to $2N$ real scalar fields, instead of writing the fits to the data as in Eq. (3.2) we write, e.g.,

$$s_{\rm median} = C_{\rm tension}(2N)^{-\alpha}\,. \tag{4.6}$$

As can be seen from the data in our tables, the various fit parameters are rather similar to those for the nonsupersymmetric case, with the most notable difference being that $s_{\rm median}$ varies as $N^{-3.16}$, compared to $N^{-2.66}$ in the non-supersymmetric case[3].

This example also illustrates the challenges of investigating random potentials for large numbers of fields. In all of our studies, supersymmetric or not, computational considerations have forced us to only probe a limited range of values of N, the number of fields, and work with truncated potentials. We are assuming that the pattern we have found, as evidenced in Figs. 1-8, will continue to hold as these constraints are relaxed.

V. A MULTIVERSE EXPLANATION OF THE COSMOLOGICAL CONSTANT?

Our results have immediate implications for attempts to find a multiverse solution to the cosmological constant problem in such field theory models. The argument for such a solution is that even if the natural scale for the cosmological constant in a typical vacuum is Planckian, one might expect to find vacua with $\Lambda \sim 10^{-120}$ in Planck units if the number of vacua is much greater than 10^{120}. Because we want a vacuum that has not only a small Λ but also a long lifetime, what we actually need is that the number of truly metastable vacua be much greater than 10^{120}.

Let us suppose that the number of vacua is $\mathcal{N}_{\rm vac} \sim \mathcal{F}^N$, with perhaps $\mathcal{F} = 10$. For metastability, we require that the tunneling exponent B be no smaller than a value $B_{\rm min}$ of

[3] Because we have not included any supersymmetry-breaking terms in the potential, the vacua here are actually stable, and our data correspond to domain walls rather than bubble walls. However, we do not expect the picture to be changed materially when the vacua are lifted.

order unity. The number of metastable vacua is then

$$\mathcal{N}_{\rm vac}\, f(B_{\rm min}) \sim \mathcal{F}^N\, e^{-\beta B_{\rm min} N^\alpha} \tag{5.1}$$

with $f(B)$ given by Eq. (3.5). The requirement that this be greater than 10^{120} can be written as

$$N - \frac{b}{\ln \mathcal{F}} N^\alpha > 120 \left(\frac{\ln 10}{\ln \mathcal{F}}\right) \tag{5.2}$$

with

$$b = \beta B_{\rm min} = \left(\frac{10^{-3}\gamma}{C_{\rm tension}}\right) \lambda B_{\rm min} \sim 10^{-3}\lambda\,. \tag{5.3}$$

This clearly needs large N, at least more than 120 if $\mathcal{F} = 10$ as in the usual analysis. The new feature here is that, because of the enhancement of the tunneling rate at large N, taking N to be too large makes matters worse rather than better. In fact, there may be no value of N for which this condition is satisfied. This is illustrated in Fig. 9, where we have taken $\alpha = 2.66$, the power we obtained from the analysis of quartic non-supersymmetric potentials. For $\mathcal{F} = 10$ the allowed values of N and b correspond to the region to the left of the solid curve. We see that there are no acceptable values of N for $b > 1.4 \times 10^{-3}$, and that the range of allowed N is relatively restricted until b falls well below this value. If instead we take $\mathcal{F} = 100$, the allowed region extends to the dashed line, with the maximum allowed b increased by roughly a factor of four.

The effect of varying the power α can be seen in Fig. 10, where we have set $\alpha = 3.16$, the value from our supersymmetric data. Although the curve is similar to that in the previous case, the values of b have fallen by more than an order of magnitude.

VI. CONCLUSIONS

Motivated by the string landscape, we have undertaken a study of the stability of vacua in multi-field quantum theories. Our study has focused on random potentials with the number of fields $N \leq 10$ and on polynomial expansions that include no more than quartic field contributions. Even with these constraints, coming from computational feasibility, the data we have accumulated provide evidence that transition rates are so rapidly enhanced as a function of N that all but an exponentially small fraction of generic local minima in such quantum field theories are unstable to rapid decay.

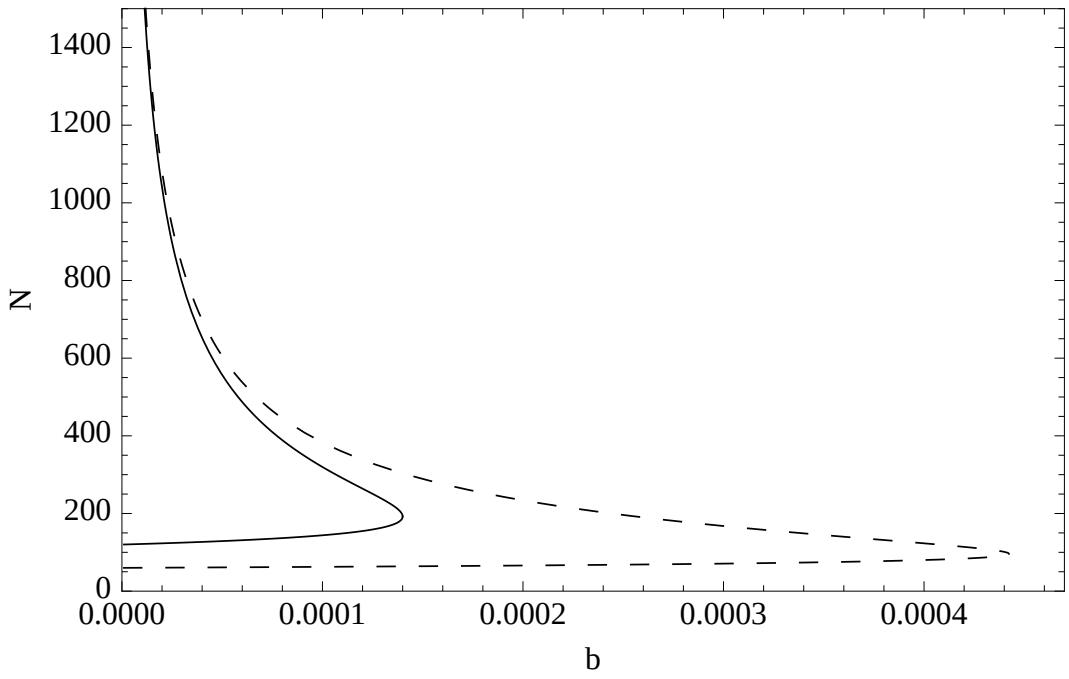

FIG. 9: Parameter ranges allowing multiverse explanations of the cosmological constant. With $\alpha = 2.66$ and $\mathcal{F} = 10$, a sufficient number of metastable vacua is only possible for parameters in the region to the left of the solid line. This region is extended to the dashed line if $\mathcal{F} = 100$.

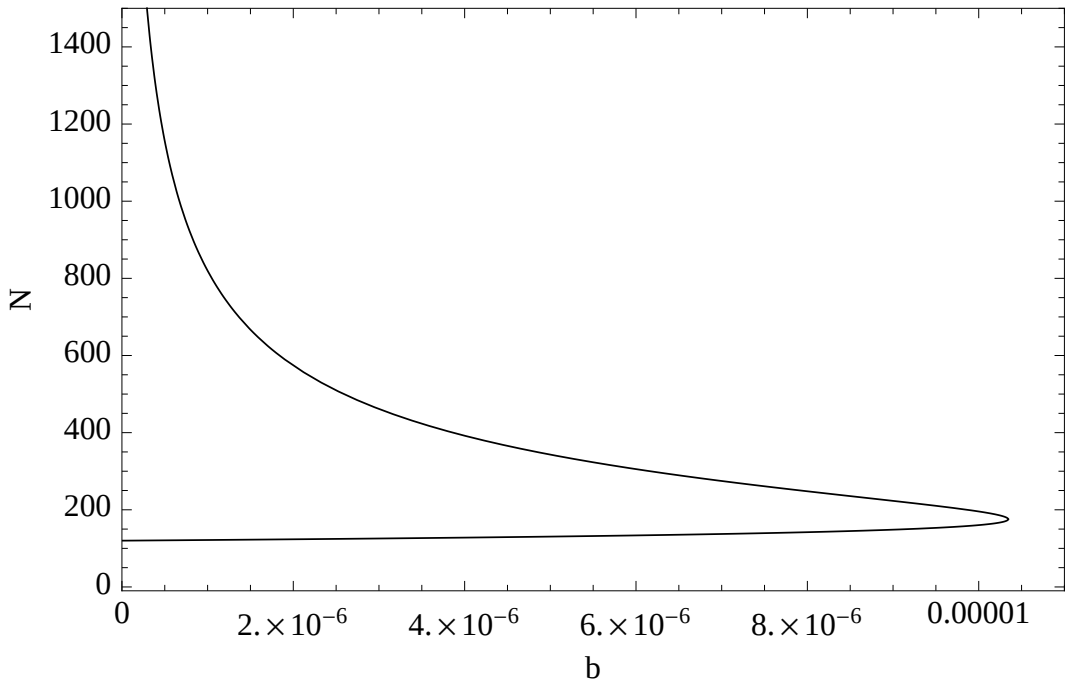

FIG. 10: Like Fig. 9, but for $\alpha = 3.16$ and $\mathcal{F} = 10$.

One consequence is that the range of parameters that give a sufficient number of metastable vacua to provide a natural solution to the cosmological constant problem is severely restricted. For example, if the moduli space dimension $N = 500$ and there are $\mathcal{F}^N = 10^{500}$ vacua, the "coupling" λ characterizing the landscape must be less than $1/20$ or so; with $N = 2000$, λ must be an order of magnitude smaller. Alternatively, if $\lambda = 1/2$ and $N = 500$, then $\mathcal{F}$ must be greater than 6×10^6.

These considerations are potentially relevant to any model invoking anthropic explanations for the cosmological constant in which the required diversity of vacua is due to the model containing a high dimensional moduli space. However, since our results have been obtained in the context of a field theory with multiple scalar fields, the impact of similar considerations on the ability of the string landscape to offer a natural solution to the cosmological constant puzzle will require further study.

Acknowledgments

We thank Pontus Ahlqvist, Robert Brandenberger, Adam Brown, Alex Chen, Frederik Denef, Zhihua Dong, Kurt Hinterbichler, Vojkan Jaksic, Dmitry Jakobson, Luchang Jin, Dan Kabat, Zhongjie Lin, Bob Mawhinney, Massimo Porrati, I-Sheng Yang, Hantao Yin, Jianglei Yu, and Daiqian Zhang for helpful discussions and comments. This work was supported in part by the U.S. Department of Energy under grants DE-FG02-85ER40237 and DE-FG02-92ER40699. Parts of the computation were carried out on Fermilab LQCD clusters.

---

[1] A. Strominger, Nucl. Phys. B **274**, 253 (1986).

[2] S. B. Giddings, S. Kachru, and J. Polchinski, Phys. Rev. D **66**, 106006 (2002).

[3] J. Polchinski, Phys. Rev. Lett. **75**, 4724 (1995).

[4] M. Grana, Phys. Rept. **423**, 91 (2006) and references therein.

[5] M. R. Douglas and S. Kachru, Rev. Mod. Phys. **79**, 733 (2007) and references therein.

[6] S. Kachru, R. Kallosh, A. D. Linde, J. M. Maldacena, L. P. McAllister, and S. P. Trivedi, JCAP **0310**, 013 (2003).

[7] A. Ceresole, G. Dall'Agata, A. Giryavets, R. Kallosh, and A. D. Linde, Phys. Rev. D **74**, 086010 (2006).

[8] M. Dine, G. Festuccia, A. Morisse, and K. van den Broek, JHEP **0806**, 014 (2008).

[9] S. Sarangi, G. Shiu, and B. Shlaer, Int. J. Mod. Phys. A **24**, 741 (2009).

[10] S. -H. H. Tye, arXiv:0708.4374 [hep-th].

[11] D. I. Podolsky, J. Majumder, and N. Jokela, JCAP **0805**, 024 (2008).

[12] A. R. Brown and A. Dahlen, Phys. Rev. D **82**, 083519 (2010).

[13] A. R. Brown, S. Sarangi, B. Shlaer, and A. Weltman, Phys. Rev. Lett. **99**, 161601 (2007).

[14] S. Coleman, Phys. Rev. D **15**, 2929 (1977) [Erratum-ibid. D **16**, 1248 (1977)].

[15] C. G. Callan, Jr. and S. Coleman, Phys. Rev. D **16**, 1762 (1977).

[16] S. Coleman and F. De Luccia, Phys. Rev. D **21**, 3305 (1980).

[17] S. W. Hawking and I. G. Moss, Phys. Lett. B **110**, 35 (1982).

[18] F. Denef and M. R. Douglas, JHEP **0405**, 072 (2004).

[19] X. Chen, G. Shiu, Y. Sumitomo, and S. H. H. Tye, JHEP **1204**, 026 (2012).

[20] D. Marsh, L. McAllister, and T. Wrase, JHEP **1203**, 102 (2012).

[21] D. Mehta, Phys. Rev. E **84**, 025702 (2011); D. Mehta, Y. -H. He, and J. D. Hauenstein, JHEP **1207**, 018 (2012).

[22] D. Mehta, to appear.

[23] F. Denef, M. R. Douglas, and B. Florea, JHEP **0406**, 034 (2004).

[24] S. Gukov, C. Vafa, and E. Witten, Nucl. Phys. B **584**, 69 (2000) [Erratum-ibid. B **608**, 477 (2001)].

[25] P. Ahlqvist, B. R. Greene, D. Kagan, E. A. Lim, S. Sarangi, and I-S. Yang, JHEP **1103**, 119 (2011).

[26] U. H. Danielsson, N. Johansson, and M. Larfors, JHEP **0703**, 080 (2007).

[27] M. C. Johnson and M. Larfors, Phys. Rev. D **78**, 083534 (2008).

[28] J. D. Brown and C. Teitelboim, Nucl. Phys. B **297**, 787 (1988).

[29] S. P. de Alwis, Phys. Rev. D **74**, 126010 (2006); S. P. de Alwis, Phys. Lett. B **644**, 77 (2007).